

# MetaHGNIE: Meta-Path Induced Hypergraph Contrastive Learning in Heterogeneous Knowledge Graphs

Jiawen Chen

jiawenchen@seu.edu.cn

School of Mathematics, Southeast University  
Nanjing, Jiangsu, China

Mengli Wei

weimengli@seu.edu.cn

School of Mathematics, Southeast University  
Nanjing, Jiangsu, China

Yanyan He

heyy@seu.edu.cn

School of Cyber Science and Engineering, Southeast University  
Nanjing, Jiangsu, China

Qi Shao

mathshaoqi@seu.edu.cn

School of Mathematics, Southeast University  
Nanjing, Jiangsu, China

Duxin Chen\*

chendx@seu.edu.cn

School of Mathematics, Southeast University  
Nanjing, Jiangsu, China

Wenwu Yu\*

wwyu@seu.edu.cn

School of Mathematics, Southeast University  
Nanjing, Jiangsu, China

Yanlong Zhao

ylzhao@amss.ac.cn

Academy of Mathematics and Systems Science, CAS  
Beijing, China

## Abstract

Node importance estimation (NIE) in heterogeneous knowledge graphs is a critical yet challenging task, essential for applications such as recommendation, knowledge reasoning, and question answering. Existing methods often rely on pairwise connections, neglecting high-order dependencies among multiple entities and relations, and they treat structural and semantic signals independently, hindering effective cross-modal integration. To address these challenges, we propose MetaHGNIE, a meta-path induced hypergraph contrastive learning framework for disentangling and aligning structural and semantic information. MetaHGNIE constructs a higher-order knowledge graph via meta-path sequences, where typed hyperedges capture multi-entity relational contexts. Structural dependencies are aggregated with local attention, while semantic representations are encoded through a hypergraph transformer equipped with sparse chunking to reduce redundancy. Finally, a multimodal fusion module integrates structural and semantic embeddings under contrastive learning with auxiliary supervision, ensuring robust cross-modal alignment. Extensive experiments on benchmark NIE datasets demonstrate that MetaHGNIE consistently outperforms state-of-the-art baselines. These results highlight the effectiveness of explicitly modeling higher-order interactions and cross-modal

alignment in heterogeneous knowledge graphs. Our code is available at <https://github.com/SEU-WENJIA/DualHNE>.

## Keywords

Heterogeneous Knowledge Graph, Hypergraph Learning, Node Importance Estimation, Contrastive Learning

## ACM Reference Format:

Jiawen Chen, Yanyan He, Qi Shao, Mengli Wei, Duxin Chen, Wenwu Yu, and Yanlong Zhao. . MetaHGNIE: Meta-Path Induced Hypergraph Contrastive Learning in Heterogeneous Knowledge Graphs. In *Proceedings of Make sure to enter the correct conference title from your rights confirmation email (WWW)*. ACM, New York, NY, USA, 12 pages.

## 1 Introduction

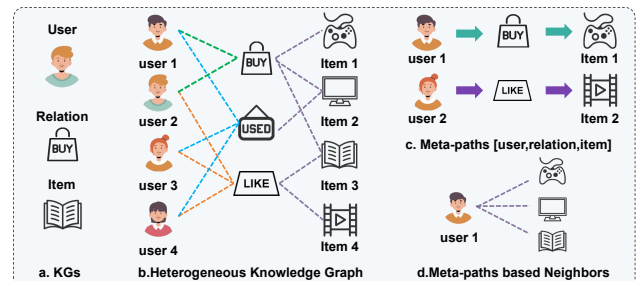


**Figure 1: Illustration of HKGs.** (a) Knowledge graph elements. (b) Heterogeneous knowledge graph. (c) Two meta-path examples (i.e., user-relation-item). (d) Users and its neighbors based on multiple meta-path.

Knowledge Graphs (KGs) have become a fundamental paradigm for representing complex, multi-typed real-world data [41, 47]. Unlike homogeneous graphs with a single type of node and edge, heterogeneous KGs incorporate diverse entities, such as users, items, authors, and movies connected by rich semantic relations [14, 39].

\*Correspondence to Duxin Chen and Wenwu Yu.

Permission to make digital or hard copies of all or part of this work for personal or classroom use is granted without fee provided that copies are not made or distributed for profit or commercial advantage and that copies bear this notice and the full citation on the first page. Copyrights for components of this work owned by others than the author(s) must be honored. Abstracting with credit is permitted. To copy otherwise, or republish, to post on servers or to redistribute to lists, requires prior specific permission and/or a fee. Request permissions from permissions@acm.org.

WWW, Dubai, United Arab Emirates

© Copyright held by the owner/author(s). Publication rights licensed to ACM.  
ACM ISBN 978-x-xxxx-xxxx-x/YYYY/MM

Within this context, a central problem is node importance estimation, which assigns importance scores to entities based on their structural and semantic roles in the graph [31, 32], such as PageRank [30] assigns importance scores to visited pages on the **World Wide Web**. Accurate and efficient NIE is essential for numerous downstream applications [1], including recommendation systems [42], expert finding [45] and information retrieval [17]. Therefore, heterogeneous information in KGs represents a relevance and diverse resource to advance recommendation system for effective ranking and retrieval.

In HKGs, entity importance often depends not only on pairwise relations but also on complex correlations between user behaviors and semantic contexts. Traditional HKG models [15, 29], which typically rely on meta-path-based neighbors in Figure 1, which captures only sequential relations between pairs of entities. This pairwise view overlooks collective interactions that naturally arise in real-world scenarios, such as a group of users jointly rating a movie or multiple authors co-authoring a paper [24, 43]. These interactions involve more than two entities and are inherently higher-order interactions. To formally capture such multi-entity relations, hypergraph modeling provides a principled way to represent higher-order structures [21], enabling more faithful estimation of entity influence. Nevertheless, existing graph neural networks (GNNs), which rely on message passing across pairwise neighbors, are fundamentally limited in encoding these multi-ary relations. The absence of unified and scalable architectures for modeling higher-order dependencies in HKGs has thus become a key bottleneck, especially the development of foundation models for knowledge-aware applications.

Existing methods have been proposed to encode structural or semantic information in HKGs [21, 29]. Techniques such as importance estimation with structural embedding of multiple entities adjusted via in-degree and similarity metrics [29, 31]. Others emphasize semantic attributes [48] integrating semantics into the representation. However, node importance depends jointly on both topological position and semantic context. Moreover, some efforts to merge the two signals usually adopt attention-based mechanisms [2, 29, 37], but these approaches often treat heterogeneous information as a homogeneous flow, without explicitly disentangling structural and semantic modalities. This leads to insufficient utilization and suboptimal extraction of heterogeneous rich information.

To address these challenges, we introduce MetaHGNIE, a novel framework for node importance estimation in heterogeneous knowledge graphs. First, to model higher-order dependencies among multiple entities, We construct a meta-path-induced hypergraph, where typed hyperedges connect all entities within a meta-path. This representation explicitly captures multi-entity interactions that conventional pairwise GNNs overlook. Second, to disentangle and integrate heterogeneous information, MetaHGNIE employs a dual-channel architecture: a structure-aware hypergraph attention network aggregates local higher-order topological features, while a semantic hypergraph transformer encodes global contextual semantics. To reduce the computational cost of dense attention, we adopt a sparse-chunked attention mechanism that efficiently processes non-zero entries. Finally, structural and semantic embeddings are fused via contrastive alignment and auxiliary supervision to ensure robust cross-modal representations. Our main contributions are summarized as follows:

- We propose a Heterogeneous Higher-Order Knowledge Graph, a meta-path-induced hypergraph framework that explicitly models multi-entity interactions. Hyperedges connect all participating entities within a meta-path, with hyperedge types encoded as ordered relation tuples, addressing the limitation of pairwise-only methods.
- We introduce a dual-channel encoding architecture that disentangles structural and semantic information: a structure-aware hypergraph attention network captures higher-order relations between multi-entities, while a contextual hypergraph transformer models semantic dependencies.
- We develop a contrastive alignment and fusion mechanism that jointly optimizes structural and semantic embeddings with auxiliary supervision, ensuring effective integration of structural and semantic embeddings for accurate node importance estimation.

## 2 Related Work

**Estimating Node Importance on Graph.** Estimating node importance in KGs is a fundamental task in graph representation learning. Existing methods can be categorized into two main paradigms: single-view approaches that focus on either structural or semantic information, and multi-view methods that attempt to integrate both. Single-view methods typically rely on GNNs and attention mechanisms. GENI [31] uses predicate-aware attention with centrality adjustment, while MultiImport [32] incorporates edge-aware attention and clustering. ILGR [29] proposes an inductive framework, and HIVEN [15] focuses on heterogeneous information. Recent works like SKES [2] combine structural centrality with optimal transport, and LENIE [26] leverages LLM-generated semantics. However, these methods are limited by their narrow perspective and fail to capture structural-semantic synergies. Multi-view methods address this by integrating multiple perspectives. MCRL [27] employs multi-view contrastive learning, LICAP [46] uses label-based contrastive pre-training, CADReN [48] introduces contextual anchors for new graphs, and EASING [3] jointly models importance and uncertainty. Yet these contrastive approaches face challenges in sample pair construction and label scarcity. This gap highlights the need for frameworks that can fully leverage heterogeneous information without heavy reliance on labels or sample selection.

**Modeling Multi-items relations in HKGs.** User-item interactions in heterogeneous knowledge graphs often involve complex multi-item relationships beyond pairwise connections. While conventional graph models capture only k-hop neighborhoods [43], they fail to represent higher-order semantic associations. Early work by Fatemi et al. [9] introduced n-ary relational structures, enabling richer group representations. Subsequent studies used hypergraphs to model multi-item interactions [23, 24, 33], with methods like ID-HAN employing hyperedge scoring [4]. Self-supervised learning techniques construct higher-order relations with user labels [19, 40, 44] but may not accurately reflect genuine meta-path based dependencies between users and items. Meanwhile, LLMs [5, 28] are also employed to learn hyper-relational knowledge graphs, but LLMs only encode semantics with unnecessary memory cost. Recent efforts have explored dual-feature fusion in hypergraph neural networks(HGNNs) [18, 38] to explore the higher-order relationships

among nodes. These works (e.g., DualHGNN [36], DPHGNN [34], and DVHGNN [22]) consider dual-channels to process images and multimedia data. However, each channel employs the same HGNNS, failing to address the structural and semantic heterogeneity in HKGs.

### 3 Preliminaries

#### 3.1 Heterogeneous Knowledge Graph

**Heterogeneous Knowledge Graph (HKGs).** A heterogeneous knowledge graph, denoted as  $\mathcal{G} = (\mathcal{V}, \mathcal{E})$ , consists of an item set  $\mathcal{V}$  and links set  $\mathcal{E} \subseteq \mathcal{V} \times \mathcal{R} \times \mathcal{V}$ . Figure 1 shows that these nodes represent diverse entities such as people, locations, or items. The edges (predicates) are triplets  $(v_h, r_i, v_t)$  that signify relationships between nodes  $v_h$  and  $v_t$  through relation type  $r_i$  from relational set  $\mathcal{R}$ .

**Meta-paths.** A meta-path  $\mathcal{P}$  is a path pattern defined as a sequence of node types and relation types in the form of  $v_1 \xrightarrow{r_1} v_2 \xrightarrow{r_2} \dots \xrightarrow{r_n} v_{n+1}$ . HKGs are rich in meta-paths, where users-items are connected with semantic path called meta-path in Figure 1(c).

#### 3.2 Meta-Path Induced Hypergraph Construction

To model multi-relation, multi-entities interactions, we propose the **Heterogeneous Higher-order Knowledge Graphs (HHKGs)** based on meta-path. Unlike meta-path neighbors in Figure 2(a)(b), which emphasize only direct connections, indirect but unobserved links (e.g., Figure 2(c)) are often overlooked, even though they reveal hidden associations between users and items. To address this, we group all users and items connected by the same relation type into a single hyperedge (Figure 3(b)), thereby describing the collective associations induced by that relation.

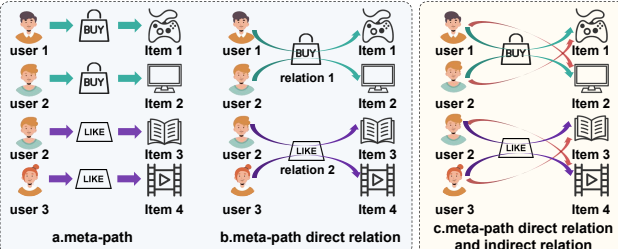


**Figure 2: Illustration of direct and indirect relations in HKGs. (a) meta-path. (b) Direct meta-path relations, e.g., observed meta-path [user<sub>1</sub>, buy, item<sub>1</sub>]. (c) Indirect meta-path relations (red arrow), e.g., unobserved meta-path as [user<sub>1</sub>, buy, item<sub>2</sub>].**

**Higher-order Relation Construction.** Given a collection of observed relational triples in the form of  $(u, r, i)$ , where  $u \in \mathcal{U}$  represents a user,  $i \in \mathcal{I}$  represents an item, and  $r \in \mathcal{R}$  denotes the relation type, we define a hyperedge  $e_r$  corresponding to multi-relation  $r$  as:

$$e_r = \{u_1, u_2, \dots, u_n, i_1, i_2, \dots, i_m\}, \quad (1)$$

where each  $(u_j, r, i_k)$  is an observed triple with relation  $r$ . This equation aggregates all users and items that are associated through the relation  $r$  into a hyperedge  $e_r \in \tilde{\mathcal{E}}$ . In HKGs, relation heterogeneity is captured by the semantic diversity of meta-paths. To preserve this property in HHKGs, we construct new hyperedge feature  $E$  by concatenating original triples. Each hyperedge is thus assigned a derived type and embedded into a feature tensor, which incorporates

heterogeneous relational semantics into the hypergraph and enriches its higher-order context. Details in Algorithm A.1.

#### 3.3 Prompt-driven Semantic Feature Extraction

Given node attributes  $\mathcal{D} = \{d_i\}_{i=1}^N$ , where each node has a name  $n_i$  and a prompt text description  $d_i$ , we also include item popularity  $p_i \in \mathbb{R}$ . A text prompt is constructed as “the description of item  $n_i$  is text<sub>i</sub>, and its popularity rating is  $p_i$ .” we compute the semantic embeddings using a pretrained language model [7]  $\mathcal{M}$ , such as BERT<sup>1</sup> and all-mpnet-base architecture<sup>2</sup>:

$$\mathbf{e}_i^{\text{sem}} = \mathcal{M}(f_{\text{concat}}(n_i, d_i)) \in \mathbb{R}^d, \quad (2)$$

where  $f_{\text{concat}}(a, b) = "a : b"$  is string concatenation. The features of all nodes are stacked as  $X_2 = [(\mathbf{e}_1^{\text{sem}})^T; \dots; (\mathbf{e}_N^{\text{sem}})^T]$  in Figure 3 (c). The final semantic encoding is obtained via a multilayer perceptron mapping layer. The semantic descriptions are encoded as data features before modeling in repositories<sup>3</sup>.

#### 3.4 Heterogeneous Higher-order Graph

**Heterogeneous Higher-order Knowledge Graph(HHKGs).** Let  $\mathcal{H} = (\mathcal{V}, \tilde{\mathcal{E}})$  denote a heterogeneous higher-order knowledge graph, consists of nodes set  $\mathcal{V}$  and hyperedges set  $\tilde{\mathcal{E}}$ . The structural features  $X_1 \in \mathbb{R}^{|\mathcal{V}| \times d_1}$  and semantic features  $X_2 \in \mathbb{R}^{|\mathcal{V}| \times d_2}$ , where  $d_1, d_2$  are the dimension of feature space. The hyperedge feature matrix is  $E \in \mathbb{R}^{|\mathcal{E}| \times d'}$ , where  $d'$  is the hyperedge feature dimension.

**Problem Definition.** Given a HHKGs  $\mathcal{H} = (\mathcal{V}, \tilde{\mathcal{E}})$  with structural feature  $X_1$ , semantic features  $X_2$  and hyperedges feature  $E$ , and observed importance score  $s \in \mathbb{R}^{|\mathcal{V}_s|}$  of subset  $\mathcal{V}_s \subseteq \mathcal{V}$ . MetaHGNIE aims to learn a score function  $S(\mathcal{V}, \tilde{\mathcal{E}}, X_1, X_2, E) \rightarrow [0, \infty)$  to predict the importance of node in HKGs.

### 4 Methodology

Existing NIE models struggle to handle higher-order relationships among multiple users and entities in HKGs, especially when faced with heterogeneous and multimodal information, resulting in limited generalization encode and ineffective fusion. To address this, we construct HHKGs and leverage LLMs to encode entity descriptions for rich semantic feature extraction. Moreover, we propose a dual-channel hypergraph contrastive learning framework that decouples structural and semantic information to generate their embeddings. Furthermore, we apply cross-modal contrastive learning and alignment to enhance intra-class compactness while preserving the distinctive nature of structural and semantic hypergraphs. Finally, we implement dual-channel prediction that integrates both structural and semantic modalities for importance estimation. Figure 3 presents the overall architecture of MetaHGNIE.

#### 4.1 Hypergraph Structural-Relational Encoding

To effectively exploit structural characteristics in HHKGs, we introduce a **Hypergraph Attention (HGAT)** mechanism that models multi-entity structural interactions for node importance estimation.

<sup>1</sup><https://huggingface.co/google-bert/bert-base-uncased>

<sup>2</sup><https://huggingface.co/sentence-transformers/all-mpnet-base-v2>

<sup>3</sup><https://anonymous.4open.science/r/MetaHGNIE-WWW26>

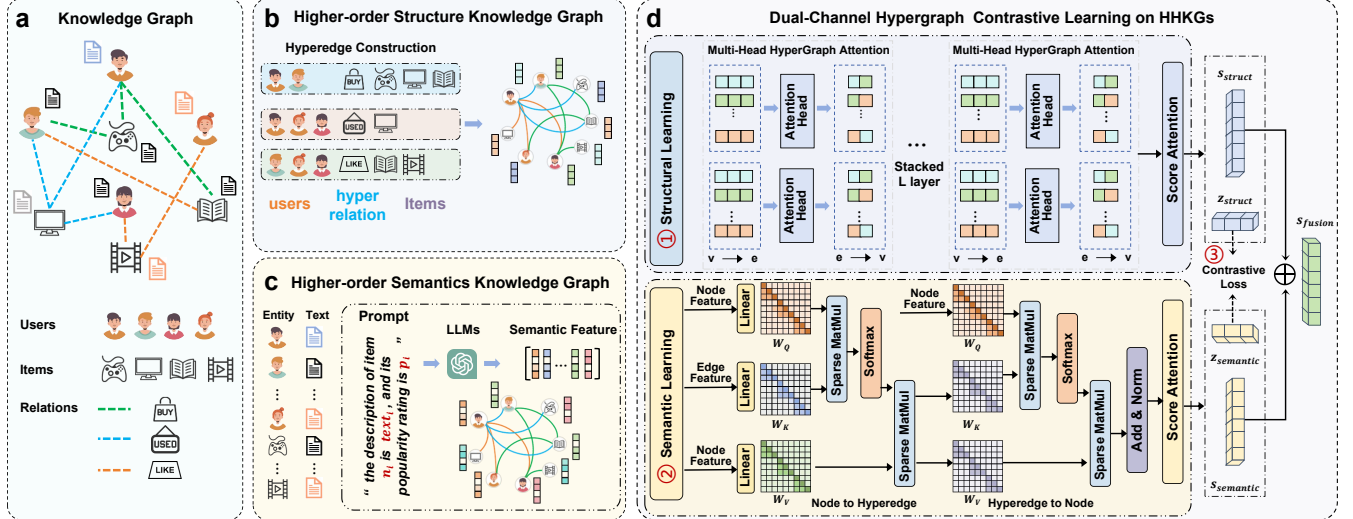


**Figure 3: Overview of the proposed MetaHGNIE framework. (a) Input heterogeneous knowledge graph. (b) Construction of the Higher-order Knowledge Graph(Sec.3.2). (c) Semantic feature extraction for Higher-order Knowledge Graph (Sec. 3.3). (d) Dual-channel encoding architecture: ①structural-relational encoder with hypergraph attention network(Sec.4.1); ②contextual-semantic encoder with sparse-chunked transformer(Sec.4.2); ③cross-modal alignment and fusion for final importance estimation(Sec.4.3).**

Messages propagate from nodes to hyperedges and then from hyperedges back to nodes. Specifically, the  $l$ -th layer contains  $d^{(l)}$  hypergraph score aggregation (HSA) heads. Let  $s_h^{(l-1)}(i)$  and  $s_h^{(l-1)}(e)$  denote the scores of node  $i$  and hyperedge  $e$  from the  $(l-1)$ -th layer, which are fed into the  $h$ -th HSA head in the  $l$ -th layer. This head aggregates the scores to produce the updated node score  $s_h^{(l)}(i)$ .

**Node-to-Relation Aggregation.** For a hyperedge  $e$  with incident nodes  $\mathcal{V}(e)$ , the aggregated score is computed as:

$$s_h^{(l)}(e) = \sum_{i \in \mathcal{V}(e)} \alpha_{ei}^{h,l} \cdot s_h^{(l-1)}(i), \quad (3)$$

where  $\alpha_{ei}^{h,l}$  is the attention weight between node  $i$  and hyperedge  $e$ . Relation between the intermediate scores of node  $i$  and hyperedge  $e$ , and the roles played by the intermediate predicate are captured by the hypergraph attention layer. This weight is computed as follows:

$$\mathcal{A}_{ei}^{h,l} = \sum_m \mathbf{a}_{h,l}^\top \left[ s_h^{(l-1)}(i) \parallel \phi(p_{ei}) \parallel s_h^{(l-1)}(e) \right], \quad (4)$$

$$\alpha_{ei}^{h,l} = \frac{\exp \left( \sigma_a \left( \mathcal{A}_{ei}^{h,l} \right) \right)}{\sum_{k \in e} \exp \left( \sigma_a \left( \mathcal{A}_{ek}^{h,l} \right) \right)}, \quad (5)$$

where  $\parallel$  denotes concatenation,  $\phi(\cdot)$  is a learnable transformation applied to the predicate  $p_{ei}$  between node  $i$  and hyperedge  $e$ ,  $\mathbf{a}_{h,l}$  is the learning parameter, and  $\sigma_a$  denotes the LeakyReLU function.

**Relation-to-Node Aggregation.** For each node  $i$ , information from its incident hyperedges  $\mathcal{E}(i)$  is aggregated as:

$$s_h^{(l)}(i) = \sum_{e \in \mathcal{E}(i)} \alpha_{ie}^{h,l} \cdot s_h^{(l)}(e), \quad (6)$$

with the attention coefficient  $\alpha_{ie}^{h,l}$  computed by:

$$\mathcal{A}_{ie}^{h,l} = \sum_m \mathbf{a}_{h,l}^\top \left[ s_h^{(l-1)}(e) \parallel \phi(p_{ie}) \parallel s_h^{(l-1)}(i) \right], \quad (7)$$

$$\alpha_{ie}^{h,l} = \frac{\exp \left( \sigma_a \left( \mathcal{A}_{ie}^{h,l} \right) \right)}{\sum_{f \in \mathcal{E}_i} \exp \left( \sigma_a \left( \mathcal{A}_{if}^{h,l} \right) \right)}. \quad (8)$$

**Multi-Head Hyper-attention Aggregation.** To capture the structural scores of nodes, each layer  $l$  employs  $d^{(l)}$  attention heads. Each head  $h$  independently computes a score via a learnable function  $\text{HSA}_h(\cdot)$  as  $s_h^{(0)}(i) = \text{HSA}_h(z_i)$ , where  $h = 1, \dots, d^{(l)}$  and  $z_i$  denotes the structural feature of node  $v_i$  initialized from  $\mathcal{X}_1$ . The initial representation is obtained by concatenating the outputs of all heads, denoted as

$$s_{\text{struct}}^{(0)} = \left\|_{h=1}^{d^{(0)}} s_h^{(0)}(i), \quad (9)$$

where  $\parallel$  denotes concatenation. Subsequently, hyper-relational information is encoded through  $L$  layers of hypergraph score attention. Each layer  $l$  performs as

$$s_{\text{struct}}^{(l)} = \text{HGAT}^{(l)}(\mathcal{H}, s_{\text{struct}}^{(l-1)}, E_{\text{feats}}), \quad (10)$$

where  $E_{\text{feats}} \in R^{m \times l_2}$  are relation embeddings derived from the hyperedges types  $\mathcal{T}(e_r)$ . Then a residual connection followed by layer normalization and feedforward network (FFN) is applied

$$s_{\text{struct}}^{(l)} = \text{Norm} \left( s_{\text{struct}}^{(l)} + \text{FFN}(s_{\text{struct}}^{(l-1)}) \right). \quad (11)$$

With  $d^{(L)}$  HSA heads in the final  $L$ -th layer, we employ the average pooling across multi hypergraph score attention heads and obtain the final representations as

$$s_{\text{struct}}^{(L)} = \text{AVERAGE} \left( s_{\text{struct}}^{(L)} \right). \quad (12)$$

Then the structural representation of embedding and prediction logits with a linear output layer :

$$\mathbf{z}_{\text{struct}} = \mathbf{s}_{\text{struct}}^{(L)}, \quad \mathbf{s}_{\text{struct}} = \text{FFN}(\mathbf{s}_{\text{struct}}^{(L)}). \quad (13)$$

This multi-head, multi-layer aggregation mechanism effectively captures higher-order interactions among nodes and hyperedges, facilitating complex structural reasoning in knowledge hypergraphs.

## 4.2 Scalable Hypergraph Semantic Encoding

To enable scalable contextual modeling in hypergraphs, it is essential to jointly model the intrinsic attributes of target nodes and the semantic contributions of hyperedge relation types. To achieve this, we propose a **Sparse-Chunked Hypergraph Transformer (SAHGT)** comprising  $L$  stacked layers, each employing a two-stage attention mechanism to capture multi-level semantic dependencies.

**Sparse-Chunked Attention.** Conventional transformer-style attention [6, 23] on hypergraphs requires constructing a dense incidence matrix  $\mathbf{H}$  and computing attention scores for all node–hyperedge pairs,  $Q_v K_e^\top / \sqrt{d}$ , where  $Q_v$  and  $K_e$  are the projected query and key vectors for node  $v$  and hyperedge  $e$ , respectively. This results in a computational complexity of  $O(NEd)$ , which becomes prohibitive for large-scale HHKGs ( $N, E \gg 10^4$ , e.g., TMDB5K, IMDB in Table A.1). To address this, we propose a Sparse-Chunk-Aggregate module that avoids dense matrix computations. The incidence matrix is stored in coordinate list (CL) format:  $\text{CL}(\mathbf{H}) = (v_i, e_i)_{i=1}^{\text{nnz}(\mathbf{H})}$ , where  $\text{nnz}(\cdot)$  is the number of non-zero entries. Attention scores are computed only over non-zero pairs and normalized via a softmax over hyperedges. Updated hyperedge messages are obtained by aggregating contributions from incident nodes:

$$h_e = \sum_{v \in \mathcal{N}(e)} \sigma_b \left( Q_{v_i} K_{e_i}^\top / \sqrt{d} \right) \cdot V_{v_i}, \quad i = 1, \dots, \text{nnz}(H), \quad (14)$$

where  $\sigma_b$  denotes the scatter softmax,  $V_{v_i}$  is the value vector of node feature, and  $\text{nnz}(H)$  is the number of non-zero entries in the incidence matrix. For enhanced scalability, we process the sparse indices in chunks of size  $C$ , enabling training on hypergraphs with millions of nodes and hyperedges without memory overflow. This approach can reduce time and memory complexity in Appendix C.

**Node-to-Hyperedge Message Propagation.** For each hyperedge  $e$ , meassage aggregates from its incident nodes  $v$  via scaled dot-product attention. Let  $\mathbf{W}_Q^{(l)}, \mathbf{W}_K^{(l)}, \mathbf{W}_V^{(l)}$  be projection matrices at layer  $l$ . The sparse attention weight from  $v$  to  $e$  is computed as:

$$\alpha_{v \rightarrow e}^{(l)} = \sigma_b \left( (W_Q^{(l)} h_v) \cdot (W_K^{(l)} h_e) / \sqrt{d} \right), \quad (15)$$

and the hyperedge representation is updated as:

$$h_e^{(l)} = \sum_{v \in e} \alpha_{v \rightarrow e}^{(l)} \cdot W_V^{(l)} h_v, \quad (16)$$

followed by multi-head concatenation and a linear output projection.

**Hyperedge-to-Node Message Propagation.** Symmetrically, each node  $v$  aggregates information from its incident hyperedges:

$$\alpha_{e \rightarrow v}^{(l)} = \sigma_b \left( (W_Q^{(l)} h_v) \cdot (W_K^{(l)} h_e) / \sqrt{d} \right), \quad (17)$$

yielding the aggregated message:

$$m_v^{(l)} = \sum_{e \in \mathcal{E}_v} \alpha_{e \rightarrow v}^{(l)} \cdot W_V^{(l)} h_e. \quad (18)$$

Then update with residual connections, Batch Normalization(BN), and a feedforward network with GELU activation:

$$h_v^{(l+1)} = \text{BN}_2 \left( h_v^{(l)} + \text{FFN} \left( \text{BN}_1 \left( h_v^{(l)} + m_v^{(l)} \right) \right) \right), \quad (19)$$

**Layer Stacking and Semantic Projection.** By stacking  $L$  layers, the model progressively refines node and hyperedge representations:

$$s_{\text{semantic}}^{(l)} = \text{SAHGT}^{(l)} (\mathcal{H}, s_{\text{semantic}}^{(l-1)}, E_{\text{feats}}), \quad (20)$$

where  $s_{\text{feat}}^{(0)} = \mathcal{X}_2$  and  $E_{\text{feats}} = E \in \mathbb{R}^{|\mathcal{E}| \times d'}$  are semantic features, hyperedge-type features, respectively. The final representation and prediction logits via a linear output layer are obtained as

$$z_{\text{semantic}} = s_{\text{feats}}^{(L)}, \quad s_{\text{semantic}} = \text{FFN}(\mathbf{s}_{\text{feats}}^{(L)}). \quad (21)$$

## 4.3 Cross-Modal Fusion with Contrastive Learning

**Fusion Mechanism.** To integrate information from structural and semantic representations, we construct an adaptive fusion mechanism to embedding  $s_{\text{fusion}}$  via adaptive combination of the two modalities:

$$s_{\text{fusion}} = \eta_1 \cdot s_{\text{struct}} + \eta_2 \cdot s_{\text{semantic}}, \quad (22)$$

where  $\eta_1, \eta_2 > 0$  and  $\eta_1 + \eta_2 = 1$  are learnable or pre-defined weighting parameters that adjust the contribution of each modality.

**Cross-Modal Alignment via Contrastive Learning.** To enhance consistency between the structural feature space and the semantic feature space  $\mathbf{z}_{\text{struct}}, \mathbf{z}_{\text{semantic}} \in \mathbb{R}^{N \times H}$ , we employ a contrastive learning strategy. The cross-modal similarity matrix is computed as  $\mathcal{S} = \mathbf{z}_{\text{struct}} \cdot \mathbf{z}_{\text{semantic}}^\top / \tau$ , where  $\tau > 0$  is a temperature parameter that modulates the similarity scores across different modalities. Here, positive pairs correspond to the embeddings of the same entity across  $\mathbf{z}_{\text{struct}}$  and  $\mathbf{z}_{\text{semantic}}$ , while negative pairs are formed by embeddings of different entities across the two modalities. The contrastive loss is defined as the symmetric average of two cross-entropy losses over the similarity matrix and its transpose

$$\mathcal{L}_{\text{contrastive}} = \frac{1}{2} [\mathcal{L}_{\text{CE}}(\mathcal{S}, \text{labels}) + \mathcal{L}_{\text{CE}}(\mathcal{S}^\top, \text{labels})], \quad (23)$$

where labels specify the index of the positive sample for each anchor, and  $\mathcal{L}_{\text{CE}}$  denotes the cross-entropy loss.

**Prediction Losses for Multi-Branch Outputs.** We apply regression supervision to three prediction branches: the structure-based output, the semantic-based output, and the fused output. Let  $\mathcal{V}' \subseteq \mathcal{V}$  be the set of training (or validation) node indices, and  $s_i$  denote the ground-truth target value for node  $i$ . The mean squared error (MSE) losses for each branch are defined as:

$$\mathcal{L}_{\text{fusion}} = \frac{1}{|\mathcal{V}'|} \sum_{i \in \mathcal{V}'} (s_{\text{fusion},i} - s_i)^2. \quad (24)$$

**Overall Objective.** The total training objective combines the fusion prediction loss, the contrastive loss, and the average of the two unimodal prediction losses

$$\mathcal{L} = \mathcal{L}_{\text{fusion}} + \alpha \cdot \mathcal{L}_1 + \beta \cdot \mathcal{L}_2, \quad (25)$$

where  $\alpha, \beta \geq 0$  are hyperparameters controlling the trade-off among different components. Here,  $\mathcal{L}_1 = \mathcal{L}_{\text{contrastive}}$  encourages the two representation spaces to be aligned through contrastive learning, promoting cross-modal consistency. Meanwhile,  $\mathcal{L}_2 = (\mathcal{L}_{\text{struct}} + \mathcal{L}_{\text{semantic}})/2$ , where  $\mathcal{L}_{\text{struct}} = \frac{1}{|\mathcal{V}'|} \sum_{i \in \mathcal{V}'} (s_{\text{struct},i} - s_i)^2$ ,  $\mathcal{L}_{\text{semantic}} =$

**Table 1: Experiments of the proposed MetaHGNIE performs compared with state-of-the-art baselines**

	FB15K		TMDB5K		IMDB		MUSIC10K	
	SPEARMAN	NDCG@100	SPEARMAN	NDCG@100	SPEARMAN	NDCG@100	SPEARMAN	NDCG@100
PR [30]	$0.350 \pm 0.019$	$0.840 \pm 0.010$	$0.625 \pm 0.013$	$0.839 \pm 0.010$	$0.561 \pm 0.006$	$0.785 \pm 0.048$	$0.177 \pm 0.019$	$0.799 \pm 0.014$
PPR [13]	$0.350 \pm 0.019$	$0.841 \pm 0.011$	$0.686 \pm 0.010$	$0.850 \pm 0.008$	$0.648 \pm 0.006$	$0.876 \pm 0.020$	$0.189 \pm 0.023$	$0.798 \pm 0.011$
HAR [25]	$0.202 \pm 0.012$	$0.826 \pm 0.005$	$0.630 \pm 0.009$	$0.814 \pm 0.021$	$0.632 \pm 0.005$	$0.795 \pm 0.036$	$0.177 \pm 0.019$	$0.799 \pm 0.014$
GCN [20]	$0.466 \pm 0.029$	$0.878 \pm 0.015$	$0.659 \pm 0.047$	$0.862 \pm 0.023$	$0.720 \pm 0.015$	$0.895 \pm 0.015$	$0.444 \pm 0.033$	$0.885 \pm 0.020$
GraphSAGE [12]	$0.753 \pm 0.009$	$0.929 \pm 0.008$	$0.547 \pm 0.032$	$0.830 \pm 0.032$	$0.705 \pm 0.020$	$0.880 \pm 0.015$	$0.459 \pm 0.020$	$0.859 \pm 0.011$
GENI [31]	$0.771 \pm 0.009$	$0.917 \pm 0.014$	$0.735 \pm 0.022$	$0.852 \pm 0.013$	$0.755 \pm 0.010$	$0.915 \pm 0.010$	$0.493 \pm 0.026$	$0.887 \pm 0.007$
LICAP [46]	$0.768 \pm 0.013$	$0.941 \pm 0.009$	$0.731 \pm 0.018$	$0.885 \pm 0.020$	$0.760 \pm 0.012$	$0.920 \pm 0.010$	$0.514 \pm 0.040$	$0.843 \pm 0.013$
HIVEN [15]	$0.774 \pm 0.015$	$0.942 \pm 0.006$	$0.760 \pm 0.008$	$0.895 \pm 0.008$	$0.748 \pm 0.006$	$0.939 \pm 0.006$	$0.546 \pm 0.012$	$0.873 \pm 0.022$
SKES [2]	$0.772 \pm 0.007$	$0.940 \pm 0.004$	$0.752 \pm 0.011$	$0.890 \pm 0.014$	$0.779 \pm 0.006$	$0.940 \pm 0.003$	$0.539 \pm 0.012$	$0.885 \pm 0.004$
HGNN [10]	$0.737 \pm 0.003$	$0.910 \pm 0.002$	$0.661 \pm 0.040$	$0.860 \pm 0.047$	$0.710 \pm 0.010$	$0.890 \pm 0.015$	$0.520 \pm 0.030$	$0.865 \pm 0.015$
HyperGAT [8]	$0.769 \pm 0.010$	$0.932 \pm 0.013$	$0.675 \pm 0.010$	$0.869 \pm 0.030$	$0.760 \pm 0.010$	$0.920 \pm 0.010$	$0.550 \pm 0.028$	$0.875 \pm 0.010$
ID-HAN [4]	$0.772 \pm 0.009$	$0.940 \pm 0.010$	$0.746 \pm 0.020$	$0.893 \pm 0.004$	$0.765 \pm 0.017$	$0.939 \pm 0.014$	$0.550 \pm 0.030$	$0.880 \pm 0.012$
DualHGNN [36]	$0.772 \pm 0.008$	$0.934 \pm 0.011$	$0.742 \pm 0.014$	$0.870 \pm 0.009$	$0.759 \pm 0.010$	$0.932 \pm 0.010$	$0.540 \pm 0.025$	$0.874 \pm 0.012$
DPHGNN [34]	$0.746 \pm 0.012$	$0.923 \pm 0.014$	$0.747 \pm 0.005$	$0.891 \pm 0.010$	$0.769 \pm 0.009$	$0.934 \pm 0.007$	$0.534 \pm 0.008$	$0.871 \pm 0.013$
DVHGNN [22]	$0.779 \pm 0.006$	$0.939 \pm 0.009$	$0.758 \pm 0.013$	$0.882 \pm 0.006$	$0.782 \pm 0.005$	$0.940 \pm 0.003$	$0.545 \pm 0.014$	$0.889 \pm 0.003$
<b>MetaHGNIE</b>	<b><math>0.787 \pm 0.004</math></b>	<b><math>0.943 \pm 0.008</math></b>	<b><math>0.762 \pm 0.003</math></b>	<b><math>0.896 \pm 0.002</math></b>	<b><math>0.793 \pm 0.004</math></b>	<b><math>0.942 \pm 0.002</math></b>	<b><math>0.552 \pm 0.034</math></b>	<b><math>0.898 \pm 0.005</math></b>

$\frac{1}{|V'|} \sum_{i \in V'} (s_{\text{semantic},i} - s_i)^2$ , represents the average of the unimodal losses, which ensures that each modality retains predictive capability.

## 5 Experiments

Our experiments are guided by the following five research questions: **RQ1**: How does MetaHGNIE perform on benchmark datasets compared with state-of-the-art methods? **RQ2**: Effectiveness of meta-path-based HHKGs in modeling multi-user and multi-item relations? **RQ3**: How does the dual-channel design contribute to performances? **RQ4**: Are all components of MetaHGNIE necessary and effective? **RQ5**: How efficient is MetaHGNIE?

### 5.1 Datasets

We include four widely evaluated real-world heterogeneous graphs, namely FB15K<sup>1</sup>, TMDB5K<sup>2</sup>, MUSIC10K<sup>3</sup> and IMDB<sup>5</sup>. For a fair comparison, we adopt the same dataset splits as in [11, 26]. The statistical properties of the dataset are shown in Table A.1 and their descriptions and details in Appendix A.1. All datasets are divided into training, validation and test as the ratio of 7:1:2.

### 5.2 Baseline Methods

To evaluate the effectiveness of the proposed framework, we compare it against a wide range of state-of-the-art methods for importance estimation, including traditional machine learning models, graph neural networks, and hypergraph neural networks. Traditional baselines include PR [30], PPR [13], and HAR [25]. Among GNN-based approaches, we consider GCN [20], GraphSAGE [12], GENI [31], LICAP [46], HIVEN [15], and SKES [2]. These methods are capable of handling unknown entities and relations in a scalable manner by leveraging structural information in heterogeneous knowledge

graphs. Similarly, to demonstrate our model’s performance in higher-order relation learning, we include hypergraph-based models, such as HGNN [10], HyperGAT [8], and ID-HAN [4]. Moreover, we select DualHGNN [36], DPHGNN [34], and DVHGNN [22], which focus on dual-channels modelling multiple modalities to enrich representations. Further implementation details for all baselines are provided in Appendix A.2.

## 5.3 Experimental Results

**5.3.1 Effectiveness of MetaHGNIE.** We benchmark the performance of MetaHGNIE and baselines on node importance estimation tasks using two ranking-oriented metrics: NDCG@100 and Spearman correlation. Higher values for both metrics indicate better performance, with NDCG@100 emphasizing the quality of top-ranked nodes and Spearman assessing global ranking. we conducted 3-fold cross-validation for these metrics across all datasets and reported the mean values and standard deviations in Table 1. with the best result in bold and the second best result underlined.

### Performance Evaluation on Node Importance Estimation.(RQ1)

Table 1 reports the performance of MetaHGNIE on heterogeneous higher-order knowledge graph compared with graph neural networks, hypergraph neural networks, and conventional machine learning methods. The results demonstrate that the proposed heterogeneous higher-order knowledge graph effectively facilitates node importance estimation. (i) On TMDB5K, MetaHGNIE again outperforms all baselines (Spearman: 0.762, NDCG@100:0.896), exceeding the previous best, ID-HAN (Spearman: 0.746) by 2.21%. (ii) On IMDB, MetaHGNIE achieves notable gains (Spearman:0.793, NDCG@100:0.942), outperforming SKES (0.779, 0.940) and LICAP (0.760, 0.920) by 1.80%/0.21% and 4.34%/2.39%, respectively, highlighting its robustness in capturing complex semantic relationships and higher-order dependencies on large-scale knowledge graphs. These results demonstrate that MetaHGNIE consistently delivers superior ranking performance across diverse benchmarks, with measurable gains over strong baselines. Its dual-branch design

<sup>1</sup><http://www.freebase.be/>

<sup>2</sup><https://www.kaggle.com/tmdb/tmdb-movie-metadata>

<sup>3</sup><https://www.kaggle.com/datasets/mexwell/10k-song-dataset>

<sup>5</sup><https://www.imdb.com/interfaces/>

effectively leverages heterogeneous higher-order knowledge graph, enabling robust and generalizable node importance estimation.

**Table 2: Performance Comparison of dual-channel models.**

	FB15K		MUSIC10K	
	SPEARMAN	NDCG@100	SPEARMAN	NDCG@100
DualHGNN [36]	$0.772 \pm 0.008$	$0.934 \pm 0.011$	$0.540 \pm 0.025$	$0.874 \pm 0.012$
DPHGNN [34]	$0.746 \pm 0.012$	$0.923 \pm 0.014$	$0.534 \pm 0.008$	$0.871 \pm 0.013$
DVHGNN [22]	$0.779 \pm 0.006$	$0.939 \pm 0.009$	$0.545 \pm 0.014$	$0.889 \pm 0.003$
DualGAT	$0.772 \pm 0.018$	$0.942 \pm 0.005$	$0.439 \pm 0.010$	$0.843 \pm 0.028$
DualGT	$0.782 \pm 0.001$	$0.934 \pm 0.013$	$0.474 \pm 0.021$	$0.865 \pm 0.014$
DualGAT-GT	$0.779 \pm 0.006$	$0.938 \pm 0.009$	$0.476 \pm 0.011$	$0.863 \pm 0.018$
DualHGAT	$0.703 \pm 0.012$	$0.924 \pm 0.008$	$0.417 \pm 0.014$	$0.854 \pm 0.010$
DualHGT	$0.765 \pm 0.013$	$0.930 \pm 0.011$	$0.471 \pm 0.021$	$0.711 \pm 0.019$
<b>MetaHGNIE</b>	<b><math>0.787 \pm 0.004</math></b>	<b><math>0.943 \pm 0.008</math></b>	<b><math>0.552 \pm 0.034</math></b>	<b><math>0.898 \pm 0.005</math></b>

### Heterogeneous High-order Knowledge Graph modeling.(RQ2)

To evaluate the benefits of our dual-channel design and meta-path induced heterogeneous higher-order knowledge graph, we compare MetaHGNIE against dual-channel baselines (DualHGNN [36], DVHGNN [22], DPHGNN [34]). We further include comparisons with dual-channel graph models (DualGAT, DualGT, DualGAT-GT) on HKGs and dual-channel hypergraph models (DualHGAT, Dual-HGT) on HHKGs. Table 2 concludes that: (i) MetaHGNIE consistently outperforms DPHGNN and DVHGNN, achieving the highest scores on both Spearman correlation (0.778) and NDCG@100 (0.943). This indicates the advantage of our integrated dual-channel architecture in leveraging complementary information. (ii) Compared to DualGAT, DualGT, DualGAT-GT on HKGs, MetaHGNIE shows notable improvements, which gains from the incorporation higher-order structures in heterogeneous graph modeling. (iii) Against Dual-HGAT and Dual-HGT model, MetaHGNIE combining HGAT and SCAHGT achieves superior performance, highlighting the benefit of a hybrid architecture. These results indicate that heterogeneous higher-order knowledge graphs more effectively capture complex structural and semantic relations between multi-users and items.

**Table 3: Evaluation of structure and semantics in MetaHGNIE.**

MetaHGNIE	FB15K		TMDB5K	
	SPEARMAN	NDCG@100	SPEARMAN	NDCG@100
Structural	$0.720 \pm 0.002$	$0.914 \pm 0.003$	$0.759 \pm 0.003$	$0.890 \pm 0.004$
Semantic	$0.709 \pm 0.004$	$0.917 \pm 0.018$	$0.613 \pm 0.018$	$0.778 \pm 0.021$
Concat	$0.731 \pm 0.003$	$0.921 \pm 0.014$	$0.739 \pm 0.009$	$0.883 \pm 0.001$
<b>MetaHGNIE</b>	<b><math>0.778 \pm 0.005</math></b>	<b><math>0.943 \pm 0.003</math></b>	<b><math>0.762 \pm 0.003</math></b>	<b><math>0.896 \pm 0.002</math></b>

### 5.3.2 Dual-channel Structure-Semantics Modeling(RQ3).

To investigate whether the proposed dual-channel design in MetaHGNIE contributes to overall model performance, we conduct an ablation study by comparing four architectural variants. The variants include: (1) *structure*, a structural prediction logits with hypergraph attention branch; (2) *semantic*, a semantic prediction logits using sparse-chunked hypergraph transformer branch; (3) *concat*, which

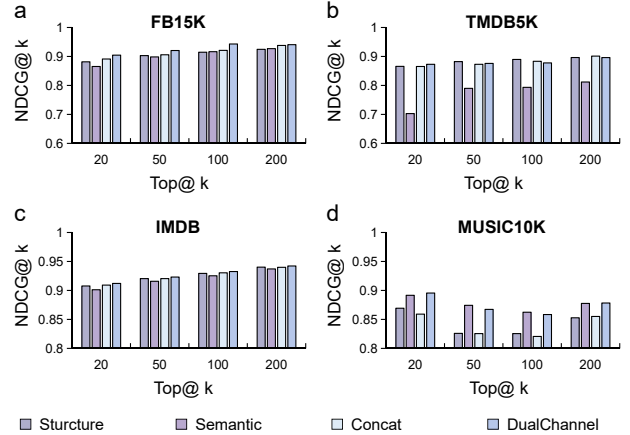


**Figure 4: Comparison of MetaHGNIE in different levels.**

combines structural and semantic feature concatenation; and (4) *MetaHGNIE*, our full model with integrated dual-branch processing.

**Performance evaluation on both structure and semantics.** Table 3 reports MetaHGNIE consistently achieves superior performance, validating the effectiveness of its dual-branch architecture that explicitly disentangles and integrates both structural and semantic information. On FB15K, MetaHGNIE achieves a Spearman score of 0.778 and NDCG@100 of 0.943, representing improvements of 8.06% and 3.17% over the structure-only model, and 9.74% and 2.84% over the semantic-only model, respectively. Compared to the concatenation-based variant, it yields gains of 6.43% in Spearman and 2.39% in NDCG@100, confirming that structured coordination outperforms simple feature fusion. For TMDB5K, the semantic-only variant performs substantially worse than the structure-only model (23.84% lower in Spearman and 14.40% in NDCG@100). Nonetheless, MetaHGNIE achieves the best performance (Spearman:0.737, NDCG@100:0.896), improving NDCG@100 by 3.10% over the best single-branch variant. These results consistently support that explicit disentanglement and joint modeling of structure and semantics significantly enhance node importance estimation.

**Performance analysis on different levels.** To further evaluate the capability of MetaHGNIE in estimating node importance across different ranking tiers, we conducted experiments on four datasets and measured NDCG@ $k$  with  $k$  varying from 20 to 200. As shown in Figure 4, MetaHGNIE demonstrates particularly strong performance at small values of  $k$ (e.g., 20 and 50), outperforming all baseline models. On FB15K, it achieves improvements over the best structural and semantic baselines, highlighting its enhanced accuracy in identifying the most critical top-ranked nodes. As  $k$  increases to 100 and 200, MetaHGNIE maintains top-tier performance, confirming its robustness across varying recommendation depths. The model consistently ranks at or near state-of-the-art levels even with longer candidate lists, illustrating its stable integration of structural and semantic signals without degradation in ranking quality. These results demonstrate that MetaHGNIE delivers superior performance across all evaluation depths, affirming that its dual-channel architecture effectively enhances both top-k ranking accuracy.

## 5.4 Module Ablation studies MetaHGNIE.

**Cross-Modal Alignment and Loss Regularization(RQ4).** Table 4 presents an ablation study of the loss components using NDCG@100. The full mode ( $L_1 + L_2$ ) consistently achieves the highest performance across all datasets, demonstrating the complementary effects of the contrastive loss ( $L_1$ ) and the unimodal prediction loss ( $L_2$ ). Removing the contrastive loss (w/o- $L_1$ ) results in a substantial performance drop, e.g., from 0.898 to 0.852 on MUSIC10K, highlighting the critical role of contrastive learning in aligning structural and semantic representations. This effect is particularly pronounced on datasets with higher modality heterogeneity, where effective cross-modal alignment is essential. Meanwhile, excluding the unimodal loss (w/o- $L_2$ ) also leads to clear performance degradation, notably on FB15K and IMDB, indicating that unimodal supervision is necessary to preserve predictive capability within individual modalities and to prevent over-reliance on cross-modal signals. Interestingly, the variant without both loss component (w/o- $L_1 + L_2$ ) occasionally outperforms the single-loss variants, suggesting some partial redundancy in how each loss regularizes the model. Nevertheless, it still underperforms the full model, confirming that  $L_1$  and  $L_2$  jointly provide complementary regularization, ensuring effective cross-modal alignment while maintaining unimodal predictive fidelity.

Table 4: Ablation study of loss function (NDCG@100)

MetaHGNIE	FB15K	TMDB5K	IMDB	MUSIC10K
$L_1 + L_2$	<b>0.943 ± 0.008</b>	<b>0.896 ± 0.002</b>	<b>0.942 ± 0.003</b>	<b>0.898 ± 0.005</b>
w/o- $L_1$	0.927 ± 0.004	0.893 ± 0.005	0.925 ± 0.009	0.852 ± 0.020
w/o- $L_2$	<u>0.934 ± 0.001</u>	0.891 ± 0.010	0.928 ± 0.011	<u>0.868 ± 0.003</u>
w/o- $L_1 + L_2$	0.935 ± 0.005	0.891 ± 0.005	<u>0.934 ± 0.004</u>	0.861 ± 0.012

**Sparse-Chunked Aggregation Mechanism(RQ4,RQ5).** To address the quadratic complexity of full attention between queries and keys in the hypergraph transformer, we introduce a Sparse-Chunked Aggregation strategy that enhances scalability on large datasets. As shown in Table 5, incorporating this mechanism leads to consistent improvements across all four benchmarks in both SPEARMAN and NDCG@100 metrics. For instance, the most notable improvement occurs on MUSIC10K, where SPEARMAN rises from 0.497 to 0.550 (+10.7%) and NDCG@100 from 0.845 to 0.878 (+3.9%). These results validate that the Sparse-Chunked Aggregation mechanism not only reduces computational overhead but also strengthens the model’s representational capacity across diverse datasets.

**Efficiency Analysis(RQ5).** Sparse-Chunked Aggregation also yields substantial efficiency gains. Results in Table 5 indicate a reduction in runtime of over 30% across all datasets, with an 84.7% decrease observed on FB15K (from 1.561s to 0.239s). GPU memory usage also decreased markedly. For example, on FB15K, runtime drops from 1.561s to 0.239s and GPU usage decreases by 49.06%; on TMDB5K, memory consumption falls by 56.12%, enabling previously infeasible configurations. These gains arise directly from chunked sparsification, which eliminates redundant computations and reduces the storage overhead of large attention matrices, making large-scale hypergraph modeling tractable.

**Parameter Analysis of Layers Number and Attention Heads.** We analyze the effect of the number of model layers and attention heads

Table 5: Evaluation Results of Sparse-Chunked Aggregation.

MetaHGNIE	SPEARMAN	NDCG@100	Time/s	GPU/G
FB15K	w/o	0.772 ± 0.002	0.936 ± 0.004	1.561
	ours	0.778 ± 0.005	0.943 ± 0.003	0.239 2.7 (+49.06%)
TMDB5K	w/o	0.751 ± 0.003	0.873 ± 0.013	2.804
	ours	0.762 ± 0.003	0.896 ± 0.002	0.518 3.3 (+56.12%)
IMDB	w/o	0.774 ± 0.013	0.938 ± 0.020	5.728
	ours	0.793 ± 0.004	0.942 ± 0.002	3.561 34.8 (+45.46%)
MUSIC10K	w/o	0.497 ± 0.015	0.845 ± 0.021	0.702
	ours	0.550 ± 0.034	0.878 ± 0.005	0.334 1.3 (+28.41%)

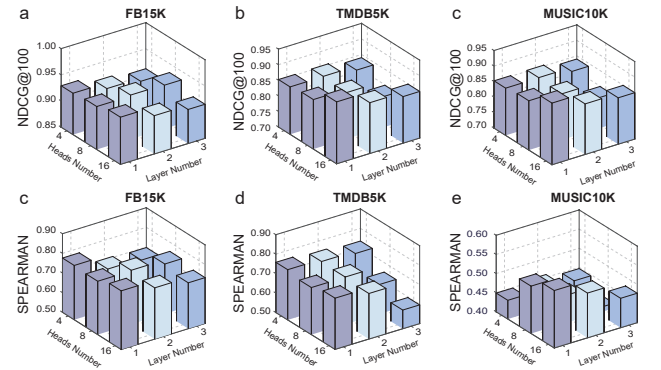


Figure 5: Ablation study of layer depth and heads’ number.

on performance in Figure 5. Increasing the number of layers leads to performance degradation. On FB15K, both NDCG@100 and Spearman remain stable with 1–2 layers but degrade notably with 3 layers (e.g., NDCG@100 drops from 0.90 to 0.79 with 16 heads; Spearman decreases from 0.80 to 0.60). On TMDB5K: 2 layers can provide slight gains over a single layer, but models with 3 layers consistently underperform. This suggests that deeper layer architectures may suffer from over-smoothing. The number of attention heads generally improve performance but at increased computational cost. On FB15K, 4–16 heads generally yield stable performance. Similarly, On TMDB5K the model achieves the best performance with 1 layer and 16 heads. However, when model combining deeper layers with more heads diminishes these gains.

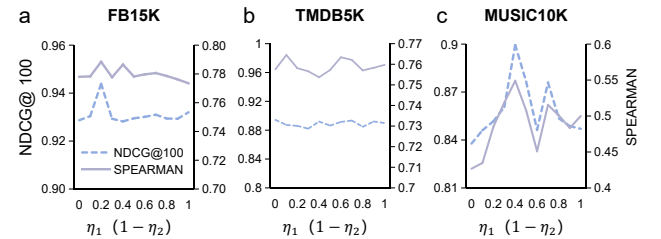


Figure 6: Hyperparameter  $\eta$  analysis of multimodal fusion.

**Parameter Analysis of Fusion and Loss Function.** Figure 6 reports the impact of parameter  $\eta_1, \eta_2$  on multimodal fusion (Eq. 22). On FB15K and TMDB5K, performance is largely insensitive to  $\eta$ : both NDCG@100 and Spearman remain essentially stable to the fusion weight. In contrast, MUSIC10K exhibits a distinct performance peak at  $\eta_1 = 0.4$ , suggesting that a moderate fusion ratio better balances ranking accuracy and correlation. We further analyze the loss

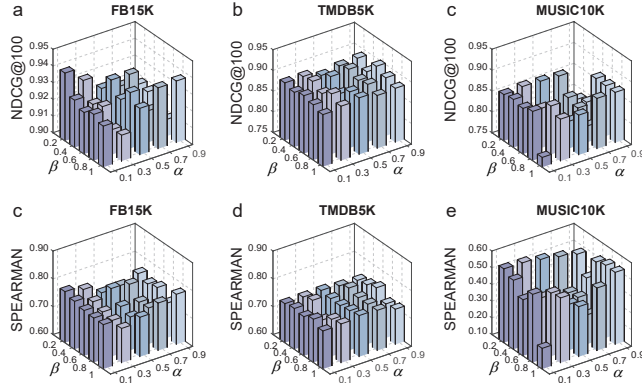


Figure 7: Hyperparameter analysis of loss function.

weighting parameters  $\alpha$  and  $\beta$  (Eq. 25), as shown in Figure 7. Results indicate that a small to moderate  $\alpha$  (0.1–0.5) generally yields higher NDCG@100 and Spearman values, implying that light contrastive regularization is sufficient to align cross-modal representations without impairing unimodal performance. Similarly, intermediate values of  $\beta$  (0.2–0.6) lead to robust outcomes. For instance, the combination of small  $\alpha$  and moderate  $\beta$  achieves the best trade-off across datasets, e.g.,  $(\alpha = 0.1, \beta = 0.2)$  on FB15K,  $(\alpha = 0.3, \beta = 0.4)$  on TMDb5K, and  $(\alpha = 0.1, \beta = 0.2)$  on MUSIC10K. Additional comparisons with alternative fusion mechanisms are provided in Appendix B.2.

## 6 Conclusion

In this paper, we propose a novel framework MetaHGNIE for node importance estimation in heterogeneous knowledge graphs. By leveraging meta-path sequences to construct higher-order relational structures, MetaHGNIE effectively captures multi-entity interactions beyond pairwise connections. The proposed dual-channel hypergraph learning approach disentangles structural and semantic perspectives through a structural-relational encoder and a contextual hypergraph transformer, while a sparse-chunked attention mechanism ensures scalability on large-scale graphs. Furthermore, the multimodal fusion strategy aligns structure and semantics via contrastive learning, yielding robust and complementary representations. Extensive experiments demonstrate that MetaHGNIE achieves superior performance on node importance estimation, validating the effectiveness of modeling higher-order dependencies and integrating structure–semantics information in heterogeneous knowledge graphs.

## References

- CHEN, D., CHEN, J., ZHANG, X., JIA, Q., LIU, X., SUN, Y., LV, L., AND YU, W. Critical nodes identification in complex networks: a survey. *arXiv preprint arXiv:2507.06164* (2025).
- CHEN, Y., FANG, Y., WANG, Q., CAO, X., AND KING, I. Deep structural knowledge exploitation and synergy for estimating node importance value on heterogeneous information networks. In *AAAI* (2024), vol. 38, pp. 8302–8310.
- CHEN, Y., WANG, T., FANG, Y., AND XIAO, Y. Semi-supervised node importance estimation with informative distribution modeling for uncertainty regularization. In *Proceedings of the ACM on Web Conference 2025* (2025), pp. 3108–3118.
- CHEN, Y., WANG, X., AND CHEN, C. Hyperedge importance estimation via identity-aware hypergraph attention network. In *CIKM* (2024), pp. 334–343.
- CHU, Z., WANG, Y., CUI, Q., LI, L., CHEN, W., QIN, Z., AND REN, K. Lim-guided multi-view hypergraph learning for human-centric explainable recommendation. *arXiv preprint arXiv:2401.08217* (2024).
- CHUNG, C., LEE, J., AND WHANG, J. J. Representation learning on hyper-relational and numeric knowledge graphs with transformers. In *SIGKDD* (2023), pp. 310–322.
- DEVLIN, J., CHANG, M., LEE, K., AND TOUTANOVA, K. BERT: pre-training of deep bidirectional transformers for language understanding. *CoRR abs/1810.04805* (2018).
- DING, K., WANG, J., LI, J., LI, D., AND LIU, H. Be more with less: Hypergraph attention networks for inductive text classification. In *EMNLP* (2020), pp. 4927–4936.
- FATEMI, B., TASLAKIAN, P., VAZQUEZ, D., AND POOLE, D. Knowledge hypergraphs: prediction beyond binary relations. In *IJCAI* (2021), IJCAI’20.
- FENG, Y., YOU, H., ZHANG, Z., JI, R., AND GAO, Y. Hypergraph neural networks. In *AAAI* (2019), vol. 33, pp. 3558–3565.
- GE, K., AND HAN, Q.-B. Node importance estimation for knowledge graphs based on multi-perspectives attention fusion mechanism. *International Journal of Pattern Recognition and Artificial Intelligence* 38, 14 (2024), 2459017.
- HAMILTON, W., YING, Z., AND LESKOVEC, J. Inductive representation learning on large graphs. *Advances in neural information processing systems* 30 (2017).
- HAVELIWALA, T. H. Topic-sensitive pagerank. In *WWW* (2002), pp. 517–526.
- HÓGAN, A., BLOMQVIST, E., COCHEZ, M., D’AMATO, C., MELO, G. D., GUTIERREZ, C., KIRRANE, S., GAYO, J. E. L., NAVIGLI, R., NEUMAIER, S., ET AL. Knowledge graphs. *ACM Computing Surveys* 54, 4 (2021), 1–37.
- HUANG, C., FANG, Y., LIN, X., CAO, X., ZHANG, W., AND ORLOWSKA, M. Estimating node importance values in heterogeneous information networks. In *ICDE* (2022), IEEE, pp. 846–858.
- HUANG, H., SUN, L., DU, B., LIU, C., LV, W., AND XIONG, H. Representation learning on knowledge graphs for node importance estimation. In *SIGKDD* (2021), pp. 646–655.
- JI, Y., WU, K., LI, J., CHEN, W., ZHONG, M., JIA, X., AND ZHANG, M. Retrieval and reasoning on KGs: Integrate knowledge graphs into large language models for complex question answering. In *Findings of the Association for Computational Linguistics: EMNLP 2024* (Nov. 2024), Y. Al-Onaizan, M. Bansal, and Y.-N. Chen, Eds., Association for Computational Linguistics, pp. 7598–7610.
- JU, W., MAO, Z., YI, S., QIN, Y., GU, Y., XIAO, Z., WANG, Y., LUO, X., AND ZHANG, M. Hypergraph-enhanced dual semi-supervised graph classification. In *ICML* (2024), JMLR.org.
- KHAN, B., WU, J., YANG, J., AND MA, X. Heterogeneous hypergraph neural network for social recommendation using attention network. *ACM Transactions on Recommender Systems* 3, 3 (Mar. 2025).
- KIPF, T. N., AND WELLING, M. Semi-supervised classification with graph convolutional networks. *arXiv preprint arXiv:1609.02907* (2016).
- LEE, J., AND WHANG, J. J. Structure is all you need: Structural representation learning on hyper-relational knowledge graphs. In *Forty-second International Conference on Machine Learning* (2025).
- LI, C., LI, T., HU, X., LUO, D., AND JIN, T. Dvhggn: Multi-scale dilated vision hgnn for efficient vision recognition. In *Proceedings of the Computer Vision and Pattern Recognition Conference* (2025), pp. 20158–20168.
- LI, J., LUO, X., LU, G., AND ZHANG, S. Hyper-relational knowledge representation learning with multi-hypergraph disentanglement. In *Proceedings of the ACM on Web Conference 2025* (2025), pp. 3288–3299.
- LI, M., LIU, K., LIU, H., ZHAO, Z., WARD, T. E., AND WU, X. Heterogeneous meta-path graph learning for higher-order social recommendation. *ACM Transactions on Knowledge Discovery from Data* 18, 8 (2024), 1–25.
- LI, X., NG, M. K., AND YE, Y. Har: hub, authority and relevance scores in multi-relational data for query search. In *Proceedings of the 2012 SIAM International Conference on Data Mining* (2012), SIAM, pp. 141–152.
- LIN, X., ZHANG, T., HOU, C., WANG, J., XUE, J., AND LV, H. Node importance estimation leveraging l1ms for semantic augmentation in knowledge graphs. *arXiv preprint arXiv:2412.00478* (2024).
- LIU, L., ZENG, W., TAN, Z., XIAO, W., ZHAO, X., ET AL. Node importance estimation with multiview contrastive representation learning. *International Journal of Intelligent Systems* 2023 (2023).
- LIU, Y., XUAN, H., LI, B., WANG, M., CHEN, T., AND YIN, H. Self-supervised dynamic hypergraph recommendation based on hyper-relational knowledge graph. In *CIKM* (2023), pp. 1617–1626.
- MUNIKOTI, S., DAS, L., AND NATARAJAN, B. Scalable graph neural network-based framework for identifying critical nodes and links in complex networks. *Neurocomputing* 468 (2022), 211–221.
- PAGE, L., BRIN, S., MOTWANI, R., AND WINOGRAD, T. The pagerank citation ranking: Bringing order to the web. Tech. rep., Stanford infolab, 1999.
- PARK, N., KAN, A., DONG, X. L., ZHAO, T., AND FALOUTSOS, C. Estimating node importance in knowledge graphs using graph neural networks. In *SIGKDD* (2019), pp. 596–606.
- PARK, N., KAN, A., DONG, X. L., ZHAO, T., AND FALOUTSOS, C. Multiimport: Inferring node importance in a knowledge graph from multiple input signals. In *SIGKDD* (2020), pp. 503–512.
- SAKONG, D., VU, V. H., HUYNH, T. T., LE NGUYEN, P., YIN, H., NGUYEN, Q. V. H., AND NGUYEN, T. T. Higher-order knowledge-enhanced recommendation with heterogeneous hypergraph multi-attention. *Information Sciences* 680 (2024), 121165.
- SAXENA, S., GHATAK, S., KOLLA, R., MUKHERJEE, D., AND CHAKRABORTY,

T. Dphgnn: A dual perspective hypergraph neural networks. In *SIGKDD* (2024), pp. 2548–2559.

[35] TANG, X., CHEN, L., SHI, H., AND LYU, D. Dhyper: A recurrent dual hypergraph neural network for event prediction in temporal knowledge graphs. *ACM Transactions on Information Systems* 42, 5 (2024), 1–23.

[36] WANG, Q., WEI, Y., YIN, J., WU, J., SONG, X., AND NIE, L. Dualgnn: Dual graph neural network for multimedia recommendation. *IEEE Transactions on Multimedia* 25 (2021), 1074–1084.

[37] WANG, X., JI, H., SHI, C., WANG, B., YE, Y., CUI, P., AND YU, P. S. Heterogeneous graph attention network. In *WWW* (2019), pp. 2022–2032.

[38] WANG, Z., CHEN, J., SHAO, Z., AND WANG, Z. Dual-view desynchronization hypergraph learning for dynamic hyperedge prediction. *IEEE Transactions on Knowledge and Data Engineering* (2024).

[39] WU, Y., LIU, X., FENG, Y., WANG, Z., YAN, R., AND ZHAO, D. Relation-aware entity alignment for heterogeneous knowledge graphs. In *IJCAI* (2019).

[40] XIA, L., HUANG, C., AND ZHANG, C. Self-supervised hypergraph transformer for recommender systems. In *SIGKDD* (2022), pp. 2100–2109.

[41] YANG, Y., HUANG, C., XIA, L., AND HUANG, C. Knowledge graph self-supervised rationalization for recommendation. In *SIGKDD* (2023), pp. 3046–3056.

[42] YANG, Y., HUANG, C., XIA, L., AND LI, C. Knowledge graph contrastive learning for recommendation. In *SIGIR* (2022), pp. 1434–1443.

[43] YIN, H., ZHONG, J., LI, R., SHANG, J., WANG, C., AND LI, X. High-order neighbors aware representation learning for knowledge graph completion. *IEEE Transactions on Neural Networks and Learning Systems* 36, 3 (2024), 5273–5287.

[44] YU, J., YIN, H., LI, J., WANG, Q., HUNG, N. Q. V., AND ZHANG, X. Self-supervised multi-channel hypergraph convolutional network for social recommendation. In *WWW* (2021), pp. 413–424.

[45] ZHANG, Q., DONG, J., CHEN, H., ZHA, D., YU, Z., AND HUANG, X. Knowgpt: Knowledge graph based prompting for large language models. *Advances in Neural Information Processing Systems* 37 (2024), 6052–6080.

[46] ZHANG, T., HOU, C., JIANG, R., ZHANG, X., ZHOU, C., TANG, K., AND LV, H. Label informed contrastive pretraining for node importance estimation on knowledge graphs. *IEEE Transactions on Neural Networks and Learning Systems* (2024).

[47] ZHANG, Z., ZHUANG, F., ZHU, H., SHI, Z., XIONG, H., AND HE, Q. Relational graph neural network with hierarchical attention for knowledge graph completion. In *AAAI* (2020), vol. 34, pp. 9612–9619.

[48] ZHONG, Z., ZHANG, Y., CHANG, Z., AND QIN, Z. Cadren: Contextual anchor-driven relational network for controllable cross-graphs node importance estimation. In *European Conference on Machine Learning and 25th Principles and Practice of Knowledge Discovery in Databases* (2025).

## A Implementation Details

### A.1 Datasets Description

**FB15K** is a subset of FreeBase<sup>1</sup>. It contains rich heterogeneous knowledge, including relational and textual information. Node importance labels are derived from the corresponding Wikipedia page views over the past 30 days.

**TMDB5K** is derived from the TMDB movie database<sup>2</sup>, containing heterogeneous nodes such as actors, crew members, and companies. Semantic information comes from movie overviews, and node importance is annotated using the official movie popularity rating. **IMDB** is processed from the IMDB database<sup>5</sup>, which contains heterogeneous graph nodes such as movies, genres, casts, crews, publishing companies, and countries. The text information of this dataset comes from IMDB movie synopsis and personal biographies. The node importance labels are derived from IMDB movie votes.

**MUSIC10K** is a music database built on the 10k song dataset<sup>3</sup> and supplemented with data from the Million Song Dataset<sup>4</sup>. It contains about 22,985 entities, including artists, songs, artist terms, and releases. Since descriptive text is unavailable, entity names are

<sup>1</sup><http://www.freebase.be/>

<sup>2</sup><https://www.kaggle.com/tmdb/tmdb-movie-metadata>

<sup>5</sup><https://www.imdb.com/interfaces/>

<sup>3</sup><https://www.kaggle.com/datasets/mexwell/10k-song-dataset>

<sup>4</sup><https://millionsongdataset.com/>

used as semantic features. Artist familiarity defines the importance of artist nodes.

**Table A.1: Datasets Details.**

	FB15K	TMDB5K	IMDB	MUSIC10K
Nodes	14951	114805	1567045	22985
Edges	592213	761648	14067776	65290
Relations	1345	34	28	8
Labeled	14105(94.3%)	4803(4.2%)	4412(19.2%)	4214 (17.6%)

**Details of Hyperedge Type Construction.** Each observed triple  $(u_j, r, i_k)$  is associated with an edge type  $r_{jk} \in \mathcal{R}$ . To characterize the derived type of hyperedges, we consider the set of all node pairs within a hyperedge  $e_r$  formed as:

$$\mathcal{P}(e_r) = \{(u_{j_p}, i_{k_q}) \mid u_{j_p} \in e_r, i_{k_q} \in e_r\}. \quad (26)$$

The corresponding set of edge types is then given by:

$$\mathcal{T}(e_r) = \{r_{j_p k_q} \mid (u_{j_p}, r_{j_p k_q}, i_{k_q}) \in \text{triples}\}. \quad (27)$$

To obtain the features of a hyperedge, we remove duplicate types from  $\mathcal{T}(e_r)$ , sort them, and encode the result as a tuple:  $\mathbf{t}_{e_r} = [r_{j_1 k_1}, r_{j_2 k_2}, \dots, r_{j_l k_l}]$ , where  $l = |\mathcal{T}(e_r)|$ . Each unique  $\mathbf{t}_{e_r}$  is mapped to a unique identifier. The hyperedge feature tensor  $\mathbf{E} \in \mathbb{R}^{|\mathcal{E}| \times d'}$  is constructed by collecting  $\mathbf{t}_{e_r}$  for all  $e_r \in \mathcal{E}$ .

**Algorithm of HHKGs Construction.** Let  $\mathcal{H} = (\mathcal{V}, \tilde{\mathcal{E}})$  denote a HHKGs, here hyperedges set  $\tilde{\mathcal{E}}$  constructed in Step 2. The structural features  $\mathcal{X}_1 \in \mathbb{R}^{|\mathcal{V}| \times d_1}$ , and semantic features  $\mathcal{X}_2 \in \mathbb{R}^{|\mathcal{V}| \times d_2}$  (see Sec 3.3), where  $d_1, d_2$  are the dimension of feature space. The hyperedge types matrix is  $\mathbf{E} \in \mathbb{R}^{|\mathcal{E}| \times d'}$ , where  $d'$  is the hyperedge feature dimension (see Step 5).

---

### Algorithm A.1 Heterogeneous Higher-order Knowledge Graph

**Require:** Triples  $\mathcal{D} = \{(u, r, i)\}$

**Ensure:** Hyperedge set  $\mathcal{E}$ , feature tensor  $\mathbf{E}$

- 1: **for** each relation  $r$  **do**
- 2:     Collect users  $\{u_j\}$  and items  $\{i_k\}$  linked by  $r$
- 3:     Form hyperedge  $e_r = \{u_1, \dots, u_n, i_1, \dots, i_m\}$
- 4:     Build pair set  $\mathcal{P}(e_r)$  of all  $(u, i)$  in  $e_r$
- 5:     Extract relation types  $\mathcal{T}(e_r)$  from triples
- 6:     Remove duplicates, sort, encode  $\mathcal{T}(e_r)$  as  $\mathbf{t}_{e_r}$
- 7:     Add  $e_r$  to  $\mathcal{E}$  and  $\mathbf{t}_{e_r}$  to  $\mathbf{E}$
- 8: **end for**
- 9: Output Hyperedge set  $\mathcal{E}$  and Hyperedge type features tensors  $\mathbf{E}$

---

## A.2 Implementation Setup

All experiments are implemented in PyTorch and executed on a workstation equipped with two NVIDIA RTX 6000 GPUs, each with 48 GB of memory. The training process is run for up to 10,000 epochs with early stopping, where the patience is set to 2000 epochs. We adopt a 3-fold cross-validation scheme to ensure robustness of the results. The default consisted of a single hidden layer with 20 hidden units. We applied an attention mechanism with a dropout rate of 0.3 to prevent overfitting. An adaptive fusion gate was incorporated to

**Table B.1: Performance of MetaHGNIE variants comparison with different levels (NDCG@k).**

	FB15K NDCG@k				TMDB5K NDCG@k				IMDB NDCG@k				MUSIC10K NDCG@k			
	20	50	100	200	20	50	100	200	20	50	100	200	20	50	100	200
Structural	0.882	0.903	0.915	<b>0.925</b>	0.866	0.882	<b>0.890</b>	0.896	0.908	0.920	0.929	0.940	0.869	0.826	0.826	0.853
Semantic	0.865	0.898	<b>0.917</b>	0.927	0.703	0.790	0.793	0.812	0.901	<b>0.916</b>	<b>0.925</b>	0.937	<b>0.892</b>	<b>0.874</b>	<b>0.862</b>	<b>0.878</b>
Concat	<b>0.891</b>	0.906	0.921	<b>0.938</b>	0.865	0.873	<b>0.883</b>	<b>0.901</b>	0.909	0.920	<b>0.930</b>	0.940	0.859	0.826	0.821	0.855
MetaHGNIE	<b>0.905</b>	<b>0.921</b>	<b>0.943</b>	<b>0.941</b>	<b>0.873</b>	<b>0.876</b>	0.878	0.896	<b>0.912</b>	<b>0.923</b>	<b>0.933</b>	<b>0.942</b>	<b>0.896</b>	<b>0.867</b>	<b>0.858</b>	<b>0.878</b>

align structural and semantic representations, and the contractive regularization size was fixed at 2000. The parameters in multi-modal fusion are initialized to  $\eta_1 = 0.3$ ,  $\eta_2 = 0.7$ , and the parameters of the regularization loss in the loss function are initialized to  $\alpha = 0.1$ ,  $\beta = 0.2$ . The model was optimized using a learning rate of 0.005 with a decay weight of  $5 \times 10^{-4}$ , and default Adam optimizer settings are used. For the baseline methods, we utilized both their originally reported results and reproduced results.

## B Ablation Study

### B.1 Ablation Study on Dual-channels

**Performance evaluation on both structure and semantics on IMDB and MUSIC10K.** The proposed dual-channel model consistently outperforms single-branch and concatenation-based baselines by jointly leveraging structural and semantic information. As shown in Table B.2, on IMDB, MetaHGNIE achieves the best performance with a Spearman correlation of 0.793 and an NDCG@100 of 0.942. This significant improvement highlights the ability of the dual-branch fusion mechanism to capture subtle inter-type dependencies that cannot be effectively modeled by either structure-only or semantics-only approaches. On MUSIC10K, MetaHGNIE again maintains superiority, reaching 0.550 in Spearman and 0.878 in NDCG@100. Although the semantic-only variant slightly surpasses the structural-only variant in Spearman correlation (0.512 vs. 0.395), both are notably weaker than the full dual-channel model. These results demonstrate that the proposed design not only provides stable improvements across datasets of different density and heterogeneity but also confirms the effectiveness of adaptive fusion in extracting complementary information from structure and semantics.

**Table B.2: Whether MetaHGNIE improves model performance**

MetaHGNIE	IMDB		MUSIC10K	
	Sperrman	NDCG@100	Sperrman	NDCG@100
Structural	0.651 $\pm$ 0.000	<b>0.934 <math>\pm</math> 0.008</b>	0.395 $\pm$ 0.054	0.826 $\pm$ 0.005
Semantic	<b>0.703 <math>\pm</math> 0.002</b>	0.940 $\pm$ 0.004	<b>0.512 <math>\pm</math> 0.007</b>	<b>0.862 <math>\pm</math> 0.007</b>
Concat	0.726 $\pm$ 0.002	<b>0.941 <math>\pm</math> 0.005</b>	0.526 $\pm$ 0.001	0.867 $\pm$ 0.007
<b>MetaHGNIE</b>	<b>0.793 <math>\pm</math> 0.004</b>	<b>0.942 <math>\pm</math> 0.002</b>	<b>0.550 <math>\pm</math> 0.034</b>	<b>0.878 <math>\pm</math> 0.005</b>

**Performance analysis on different levels.** Table B.1 shows the details of NDCG@ $k$  ( $k = 20, 50, 100, 200$ ) scores comparison on four datasets. The results consistently show that regardless of  $k$ , MetaHGNIE achieves the highest or near-highest NDCG@ $k$  scores, indicating its robustness on score lists of different lengths.

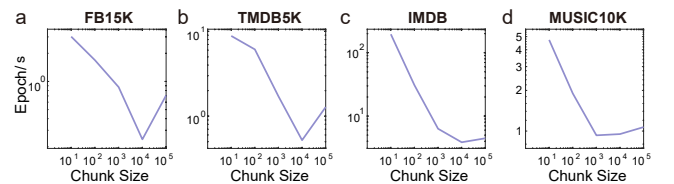
**Table B.3: Evaluation of different fusion mechanisms**

	FB15K		TMDB5K	
	NDCG@100	SPEARMAN	NDCG@100	SPEARMAN
Adaptive	<b>0.943 <math>\pm</math> 0.005</b>	<b>0.787 <math>\pm</math> 0.003</b>	<b>0.886 <math>\pm</math> 0.003</b>	<b>0.760 <math>\pm</math> 0.004</b>
Attention	0.920 $\pm$ 0.003	0.749 $\pm$ 0.016	0.860 $\pm$ 0.017	0.733 $\pm$ 0.013
Concat	<b>0.930 <math>\pm</math> 0.003</b>	<b>0.771 <math>\pm</math> 0.012</b>	<b>0.885 <math>\pm</math> 0.006</b>	<b>0.747 <math>\pm</math> 0.009</b>
Fixed	0.931 $\pm$ 0.003	0.774 $\pm$ 0.004	0.868 $\pm$ 0.014	0.723 $\pm$ 0.005
Gate	0.919 $\pm$ 0.003	0.752 $\pm$ 0.019	0.883 $\pm$ 0.009	0.750 $\pm$ 0.015

### B.2 Ablation Study on Gate mechanism

**Impact of different fusion designs on structural and semantic integration.** We conduct an ablation study to evaluate the effectiveness of various fusion mechanisms in integrating structural and semantic embeddings (Eq.22). As summarized in Table B.3, the proposed *adaptive gate* mechanism consistently achieves the highest performance across both FB15K and TMDB5K datasets, with NDCG@100 scores of 0.94 and 0.886, and Spearman correlations of 0.787 and 0.760, respectively. These results notably outperform those of alternative fusion strategies, including attention-based, concatenation, fixed-weight summation, and simple gating mechanism.

The superior performance of the adaptive gate can be attributed to its ability to dynamically balance the contributions of structural and semantic modalities in an instance specific manner. Unlike static or heuristic fusion approaches, such as the fixed-weight method, which applies a pre-defined ratio to combine features, or concatenation, which often introduces redundancy and noise—the adaptive gate learns to emphasize the more informative modality conditioned on each input. This flexibility is especially critical in heterogeneous knowledge graphs, where the relative importance of structural and semantic signals may vary substantially across nodes and relations. The consistent gains observed across both ranking metrics and datasets confirm that adaptive gating provides the most effective and instance-specific fusion for MetaHGNIE.

**Figure C.1: Runtime(s) of SCA with chunk size( $10^1$  to  $10^6$ ).**

**Table C.1: Calculation memory consumption (GPU/GB). Best values (**bold**) and second-best (underlined).**

	FB15K		TMDB5K		IMDB	
	struct	semantic	struct	semantic	struct	semantic
GNIE	<u>1.8</u>	<u>2.8</u>	3.0	10.7	41.3	46.5
RGTN	3.5	4.7	4.7	11.7	53.1	55.9
MetaHGNIE(w/o-SCA)	2.6	3.8	<u>2.3</u>	<u>5.6</u>	<u>39.8</u>	48.2
MetaHGNIE(SCA)	<b>0.6</b>	<b>1.1</b>	<b>2.0</b>	<b>3.1</b>	<b>26.1</b>	<b>32.3</b>

## C Complexity Comparison

**Sparse-Chunked Attention Analysis.** Conventional hypergraph attention [35] constructs a dense incidence matrix  $\mathbf{H} \in \{0, 1\}^{N \times E}$  and computes scores for all node–hyperedge pairs, leading to  $O(NEd)$  complexity. We propose a *Sparse-Chunk-Aggregate (SCA)* module that operates directly on the sparse COO form of  $\mathbf{H}$ , computing attention only on nonzero entries and normalizing via scatter-softmax. This reduces both computation and memory by a factor

of  $\rho = \text{nnz}(\mathbf{H})/(NE)$  while avoiding zero-padding. Therefore, complexity drops from  $O(NEHd)$  to  $O(\text{nnz}(\mathbf{H})Hd)$ , with softmax reduced from  $O(NE)$  to  $O(\text{nnz}(\mathbf{H}) \log k)$ , where  $k$  is the average node degree. Thus, SCA achieves linear savings in  $\rho$  without sacrificing attention expressivity. By processing  $\mathbf{H}$  in chunks size  $C$ , we avoid allocating large  $[N \times E]$  tensors or global COO arrays that may exceed CUDA’s  $2^{31} - 1$  index limit. SCA reduces overall memory usage. Since the total number of nonzero elements is unchanged, memory consumption does not depend on the chunk size  $C$ , whereas runtime does.

We also compare GPU consumption of structural and semantic channels across four models: the graph attention network GNIE [31], the graph Transformer RGTN [16], MetaHGNIE without SCA, and MetaHGNIE with SCA, under identical training settings (Table C.1). On FB15K, MetaHGNIE(SCA) reduces GPU usage to 0.6 (structural) and 1.1 (semantic), saving 65–80% compared to GNIE (1.8, 2.8) and RGTN (3.5, 4.7). On IMDB, savings remain substantial: SCA lowers structural/semantic costs from 41.3/46.5 (GNIE) and 53.1/55.9 (RGTN) to 26.1/32.3, achieving 35–50% reduction. These results demonstrate that SCA effectively eliminates redundant computation by processing only nonzero entries, enabling MetaHGNIE to maintain expressiveness while substantially improving efficiency.